



UNIVERSITY OF LEEDS

This is a repository copy of *Monitoring deformation of small scale model tunnels under load testing*.

White Rose Research Online URL for this paper:  
<http://eprints.whiterose.ac.uk/123927/>

Version: Accepted Version

---

**Article:**

Chen, H-M, Smith, M, Yu, H-S et al. (1 more author) (2014) Monitoring deformation of small scale model tunnels under load testing. *Survey Review*, 46 (339). pp. 417-425. ISSN 0039-6265

<https://doi.org/10.1179/1752270614Y.0000000122>

---

This is an Accepted Manuscript of an article published by Taylor & Francis in *Survey Review* on 29 Oct 2014, available online:  
<https://doi.org/10.1179/1752270614Y.0000000122>

**Reuse**

Unless indicated otherwise, fulltext items are protected by copyright with all rights reserved. The copyright exception in section 29 of the Copyright, Designs and Patents Act 1988 allows the making of a single copy solely for the purpose of non-commercial research or private study within the limits of fair dealing. The publisher or other rights-holder may allow further reproduction and re-use of this version - refer to the White Rose Research Online record for this item. Where records identify the publisher as the copyright holder, users can verify any specific terms of use on the publisher's website.

**Takedown**

If you consider content in White Rose Research Online to be in breach of UK law, please notify us by emailing [eprints@whiterose.ac.uk](mailto:eprints@whiterose.ac.uk) including the URL of the record and the reason for the withdrawal request.



[eprints@whiterose.ac.uk](mailto:eprints@whiterose.ac.uk)  
<https://eprints.whiterose.ac.uk/>

# MONITORING THE DEFORMATION OF SMALL SCALE MODEL TUNNELS UNDER LOAD TESTING

**Han-Mei Chen, Martin Smith, Hai-Sui Yu, and Nikolaos Kokkas**  
The University of Nottingham, UK

## ABSTRACT

This paper describes a study to assess the suitability of two non-contact methods of measurement used to monitor a series of small scale model tunnels built to different specifications that are being subjected to load testing. The model tunnels are being built to validate mathematical modelling techniques. Presented here are the results to assess the suitability and quality of survey results based on photogrammetry and laser scanning. The two key parameters to be measured are the deformation that is created in the tunnel (distance measurement) and the length and width of cracks.

Results showed that both the remote measurement techniques were suitable for the measurement of the small model tunnels and compared well against appropriate potentiometer and vernier calliper measurements.

**KEYWORDS:** Laser scanner, photogrammetry, condition monitoring, deformation, physical models, tunnel stability.

## INTRODUCTION

There are many brick-lined tunnels in the UK serving a variety of purposes from railways to sewers. Whatever their purpose they are subjected to degradation such as spalling, perished mortar and loose bricks during their service life. Ground stress and movement can cause significant deformations to the tunnel structure and lining. If this goes unnoticed and without remedial maintenance severe disruption to the tunnel use can occur. Regular and frequent monitoring to diagnose any deterioration is of major importance. Decision making can be supported by numerical modelling to analyse and predict mechanical behaviour of the tunnel.

Traditionally visual inspection and manual contact methods have been used which provide a variable standard of quality and subjective judgement. Direct contact measurements using simple steel tapes and tape extensometers (Kolymbas, 2005) can be extremely time consuming to use. Haack et al. (1995) used the methods of georadar, infrared thermography and multispectral analysis for tunnel applications using an experimental wall. This work showed that there are benefits in using all three methods under certain circumstances.

The monitoring of the geometric shape of tunnels has always provided a challenge for the surveying community. Their size and shape has required 3D measurements to be collected to enable a full understand of the tunnel geometry. In the past, this has been split often into a cross sectional shape and a longitudinal direction. The long narrow nature of most tunnels provides limited scope for some forms of survey measure where as it can be difficult to achieve a strong survey geometry.

Gyro-theodolites and more recently inertial positioning systems have been useful tools in working underground. The remote measurement techniques of laser scanning and digital photogrammetry have been thought of as potentially useful methods having been used in many natural environment and engineering applications for example Guarnieri et al, (2004) and Turner et al. (2006).

An alternative approach to physical measurement is to use numerical modelling and a number of approaches for old tunnel masonry structures have been proposed (Idris et al, 2008 and 2009). However, the modelling and analysis of the mechanical behaviour of existing brick-lined tunnels remains challenging. It is extremely difficult to study tunnel behaviour on a 'working tunnel' to fully understand the influencing factors and components, due to a whole range of factors such as; practical health and safety issues, complex material components, and uncontrollable experimental environment. So to undertake this type of study a series of small scale model tunnels were built and tested under laboratory conditions. During the tests, advanced monitoring techniques such as laser scanning and photogrammetry were used to record tunnel deformation and lining defects, which were designed to substitute or supplement the conventional manual procedures. In the wider scope of the project, the physical trials were used to validate numerical models that were developed. This would enable the numerical models to be used for real world field studies to enable accurate prediction of the actual behaviour of a masonry tunnel.

It is noted that these physical model tests are not required to replicate the real tunnels with various conditions, but should provide similar boundary and loading conditions, which can be easily measured and assessed.

### Aims and objectives

The general aim of the trials presented in this paper is to develop a surveying methodology for the measurement of small scale tunnels to monitor the deformation and crack sizes while they are being load tested under laboratory conditions.

The objectives are:-

1. Understand the background to the design and building of the model tunnels and the loading strategy to enable the prediction of the nature and position of the expected movement and failure.
2. Design of a measurement system based on laser scanning, digital close range photogrammetry and linear potentiometers. These three methods produce very different output for deformation analysis, so by using the three techniques it is possible to study how well they complement each other as well as providing verification of their results. The laser scanning will produce a 'cloud' of points with known 3D coordinates suitable for surface reconstruction. The proposed photogrammetric solution will be based on high precision target point coordination for 3D point movement analysis while the potentiometers will only provide a distance measurement in one direction.
3. Develop a suitable method for presentation of the results and an analysis of results obtained.

### THE DESIGN AND BUILDING OF THE MODEL TUNNELS

#### Required trials - an engineering perspective

The aim of the engineering study was to gain an understanding of the mechanical behaviour of masonry tunnels. There were many variables in the design and construction and possible loading strategies of these tunnels so it was important to identify beforehand what the significant factors would be and which of these would be the feature of this study.

Some of the influences on the behaviour of these tunnels included:-

1. brick bond pattern;
2. the water content of the surrounding soil;

3. brick variability;
4. mortar variability;
5. surrounding soil type;
6. types of load e.g. concentrated and uniformly distributed loads.

The engineering decision was to investigate the effect of varying mortar mix proportions and the types of loading (although only one type of loading is presented here). All the other parameters were kept constant for each model tunnel built and tested.

Considering the effect of these two variables on the predicted behaviour of the tunnel and therefore the design of the measurement process it was decided that the same measurement method could be employed for all trials.

### Model tunnel design and construction

There are a number of key components in the design and construction of the model tunnels. The tunnel lining was to be made of brick which needed to be surrounded by soil. To retain the soil a rigid box made mainly of wood was constructed with a Perspex facing over the outer 2 layers of the brick lining exposed at the front and rear. Fig. 1 shows a sketch of the design and dimensions of the models constructed. A plastic sheet was used as a liner to stop the soil falling between the Perspex and the bricks (nominal 2mm gap) and also assisted in reducing the friction between the soil and the box when the loading was applied. To increase the stiffness a set of hot finished square and rectangular hollow section steel beams were designed and bolted at either side of the box see Fig. 2.

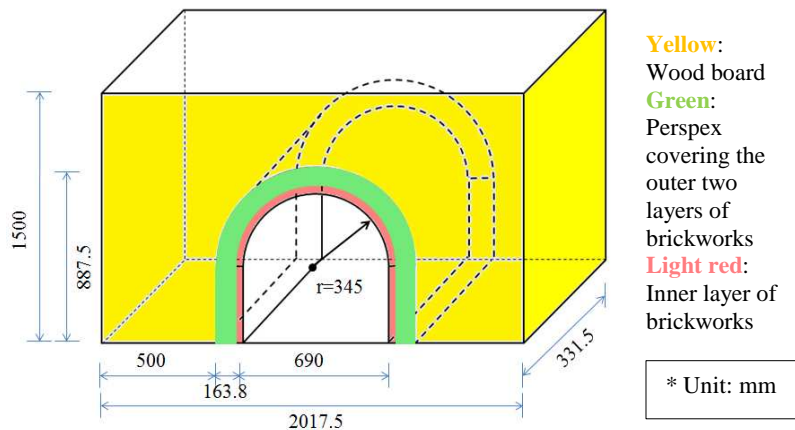


Fig 1. The rigid box surrounding the brick-lined tunnel (Chen, 2014, Chen et al, 2013)

The brick arches were made from half size bricks  $107.5 \times 51.3 \times 32.5$  mm with a nominal 5mm joint. The arch consisted of three layers of similar sized bricks and stretcher bond brickwork where appropriate as shown in Fig. 3.

The strength of the mortar was varied appropriately for each trial as this was one of the variables being investigated. As an example, the first physical model had a comparatively higher strength mortar mix comprising cement, lime and sand in respective proportions of ratio 1:1:6 as prescribed by BS 4451:1980 (1980).

The aim was to try and simulate the behaviour of deep seated tunnels (e.g. mountain tunnels) so a uniform load was subjected to the physical model. Monotonic load tests were run through the research consisting of one loading frame and a long cross beam to hang two hand-operated ‘Enerpac’ jacking systems associated with two load cells as shown in Fig. 2.

The load from two jacks was applied evenly on the whole surface of the overburden soil by a load spreader beam (1690 × 150 × 250 mm, L × W × H) with 5 point loading rollers (equally distributed along the length of the box), and a 20 mm thick steel plate of 1950 mm long and 300 mm wide underneath, as can be seen in Fig. 2.



Fig 2. Loading system installation for uniform load (Chen, 2014)



Fig 3. The brick-lining of the tunnel (Chen, 2014)

The soil fill was Portaway sand compacted in nominally 125mm layers thickness and compacted with a standard 2.5 kg compaction test drop hammer for 20 times. The final depth was 1075mm from the tunnel toe. Fig. 2 shows the uniform loading system of the prepared tunnel.

## TUNNEL MONITORING

### Methodology

The monitoring of the tunnel was undertaken through three different technologies; laser scanning, photogrammetry and the use of potentiometers. Each of these technologies offered benefit as well as enable some comparison of techniques to be undertaken. Vernier callipers were also used for some direct crack measurements.

It was planned to load each tunnel in 10kN stages and at the end of each stage measurements were taken thus building up the picture of the changes in shape until a failure point is reached. Loads were sustained for 1 to 2 minutes to enable the measurements to be made.

The three techniques used offer three different data sets;

1. The laser scanner was providing a very high resolution point cloud of 3D coordinates of the surface measurements.
2. The photogrammetry measurements were providing coordinates of discrete targeted points in the first instance, although there is the potential for further natural detail points to be measured at a later stage.
3. The linear potentiometers (POT) were installed at the predicted failure points.

#### Equipment, observations and processing

The FARO Focus<sup>3D</sup> laser scanner (Faro 2011) was used which only required some consideration of the best positioning before loading and then measurements could be made very easily at each epoch. The scanning took place on only one side of the tunnel and focussed on very high resolution/density of point distribution. The density of the points was 6 points per square cm which was chosen to ensure the cracking could be detected at an early stage. The setting up and recording of the scanner measurements was easy and efficient and required only about a minute to complete. Fig. 4 shows a picture of the scanner.



Fig 4. The front view of the laser scanner FARO Focus<sup>3D</sup>

The cloud of 3D coordinated points produced by the laser scanner was processed using Geomagic Studio 10 (Geomagic, 2007) and a work flow is given in Fig. 5. Only the points around the tunnel were extracted from the full 360° scans automatically produced by the Faro scanner.

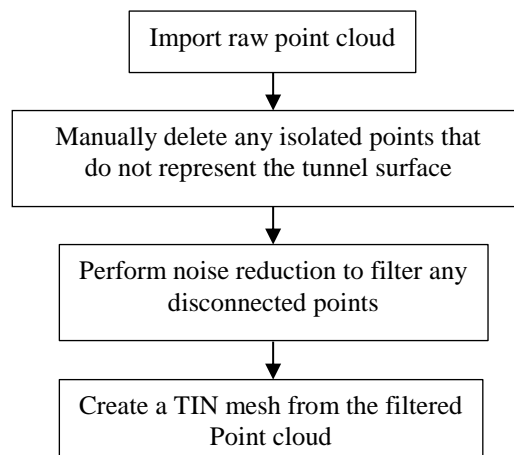


Fig 5. The work flow for processing the 3D point cloud through Geomagic Studio 10

A process of triangulating a mesh surface from the filtered point cloud is the final stage that represents the reconstructed tunnel. The mesh consisted of approximately



300K three dimensional triangles. Fig. 6 shows the filtered point cloud on the left and the reconstructed mesh on the right.

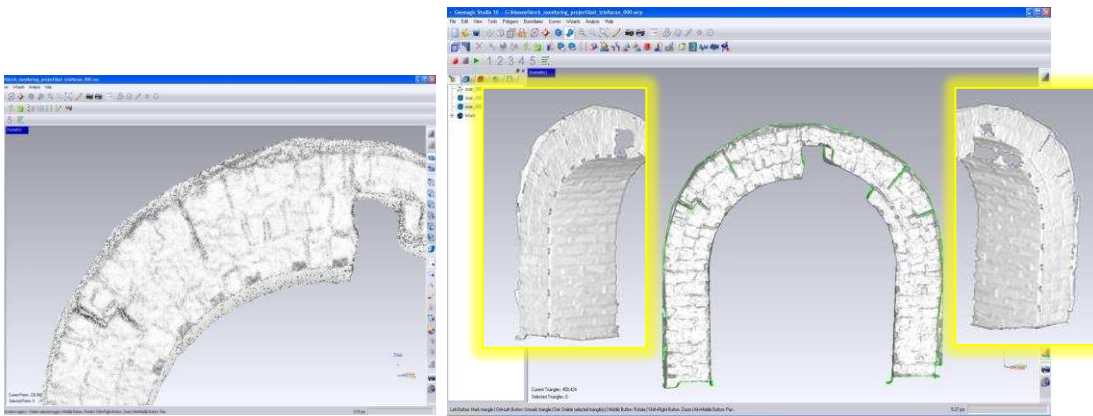


Fig 6. Extract from 3D point cloud model (left, unwrapped; right, wrapped) (Chen, 2014)

Appropriate crack measurements were then be made on the ‘wrapped’ object which were compared with traditional vernier calliper measurements see Fig. 7 and results section.

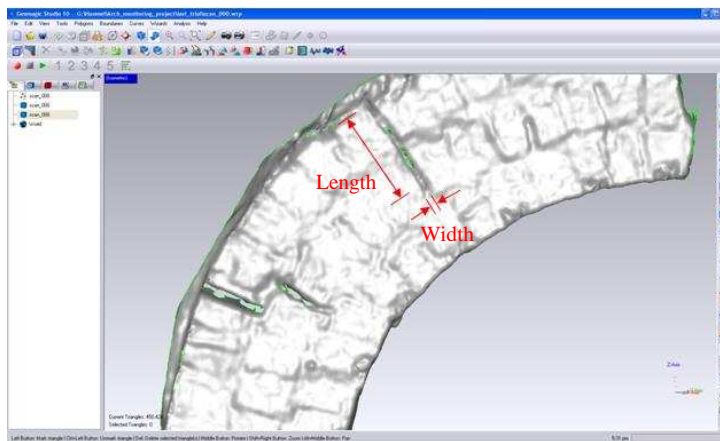


Fig 7. 3D tunnel model after wrapping with crack width and length measurement (Chen, 2014)

In addition, a three dimensional object comparison for all the nodes in the 3D meshes produced at different loadings was performed and the resulting three dimensional deviation maps are shown in Figures 14 and 15.

The photogrammetric measurement was based on images captured from a Canon EOS-5D Mark II 21 megapixel digital single lens reflex camera (see Fig. 8). While the photogrammetry processes can consider discrete targets as well as digital surface models, it was decided that discrete target coordination would be the most accurate approach. So, approximately 150 reflective markers were installed to define control points and movement detection points. They were installed primarily on the first tunnel lining ring (intrados) on both openings of the tunnel. As these targets were retro reflective they relied on the use of flash to illuminate them which meant less reliance was placed on good ambient light.



Fig 8. The top view and the front view of Canon EOS-5D Mark II

Initially a camera calibration process is necessary in order to determine accurately the geometric characteristics of the camera including any lens distortions. Determining the camera calibration parameters will enhance the accuracy of any measurements performed on the tunnel surface. The camera calibration was performed using Australis (version 7.0, see Australis Guide (Photometrix Pty Ltd., 2006)) with 25 images of a calibration frame (Fig. 9). Each image was taken from a different position and orientation while the optical axis of the camera was pointing towards the centre of the calibration frame.

Calibration process involves an automatic measurement of the retro-reflective targets positioned on the calibration frame and a subsequent bundle block adjustment using the extended collinearity equations. The camera calibration process estimates the camera parameters (see Table 1 and Fig 10) as well as all the exterior orientation parameters for each picture.



Fig 9. Camera calibration frame

Table 1. Camera calibration parameters

Parameter	Value (mm)	Standard deviation (mm)
$f$	29.760	0.057
$x_o$	-0.211	0.054
$y_o$	0.074	0.093

The lens distortions were calculated as a function of the radial distance away from the centre of the CCD chip. The lens distortion curves are represented in Fig. 10.



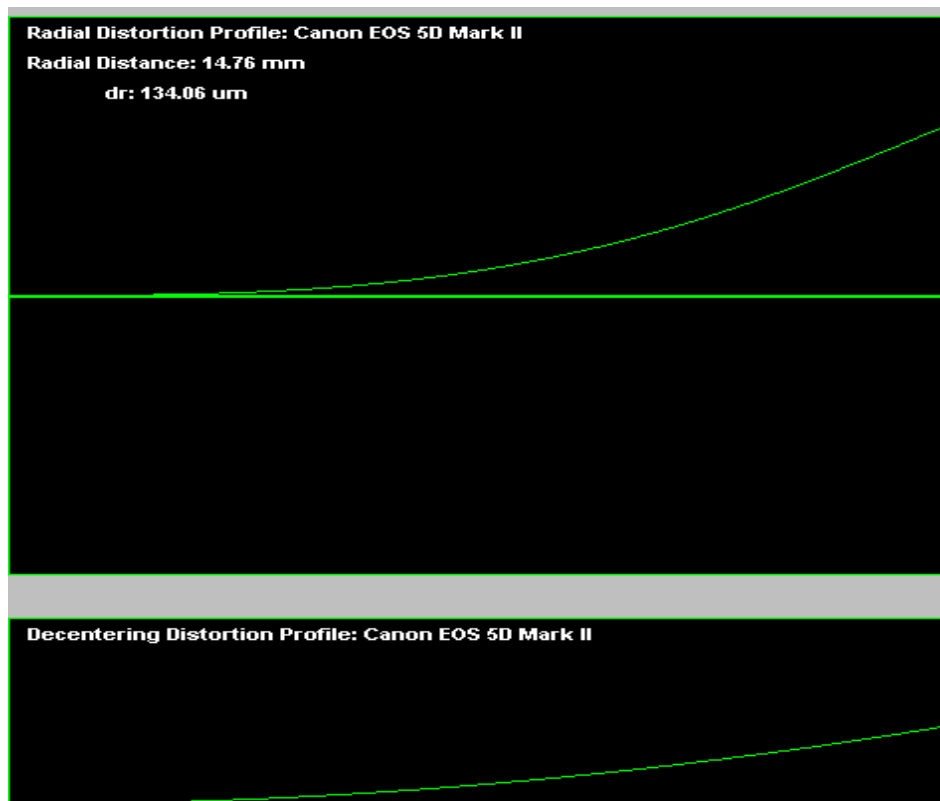


Fig 10. Lens distortion curves

Once the calibration of the camera is complete the parameters are utilised to process the images of the tunnel. The workflow used is based on the collinearity equations (bundle adjustment), see Fig. 11. An important point in the process was the capture suitable images of the target points. Each point must be recorded on at least two images to provide an intersection and as many coded targets as possible should be recorded on as many images as possible. The coded targets enabled the network of images captured to be automatically matched and target points measured. The use of automatic point measurement enabled a very high precision of measurement to be obtained typically reaching  $9\mu\text{m}$ . Fig. 12 shows a screen shot from Australis showing some measured images at a failure point and the tunnel as a 3D point cloud. The scaling is performed with the introduction of a carbon fibre metrology scale bar (shown in red in Fig. 12). To enable comparisons between different loading strategies the initial 'non-loaded' coordinate system was used as the benchmark on which the deformed point clouds is transformed. All the coordinate analysis was performed in Microsoft Excel.

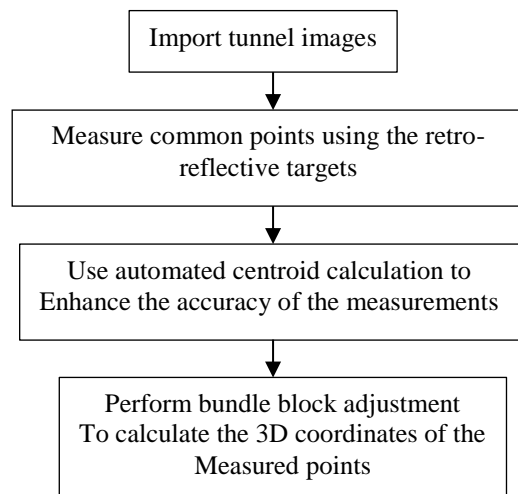


Fig 11. Australis summary work flow for measuring 3D points on the tunnel images

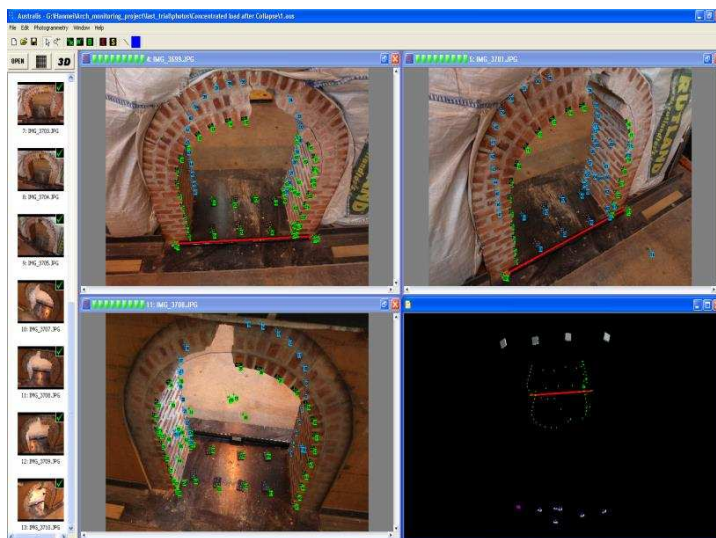


Fig 12. Australis screenshot showing 3D photogrammetric network from multiple images and the 3D view (Chen, 2014, Chen et al, 2013)

The linear potentiometers as shown in Fig. 13 enable the movement in the direction of the potentiometer to be determined and this gives a direct distance.



Fig 13. Linear potentiometer (Chen, 2014)

## RESULTS AND DISCUSSION

### Measurement of the crown

Fig. 14 and Fig. 15 show an example of the 3D views of the tunnel crown in different colours produced from 3D Compare, showing the displacement between images at 0kN and 551kN load. The maximum deformation was at the crown around 30mm. The deformation gradually reduced towards the springing of around a minimum of 2mm.

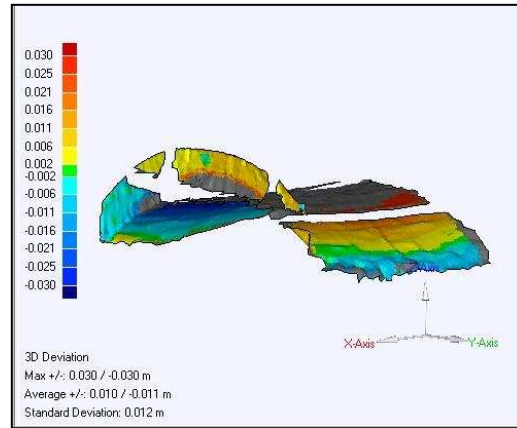


Fig 14. The side view of the 3D deviation of the tunnel crown (Chen, 2014)

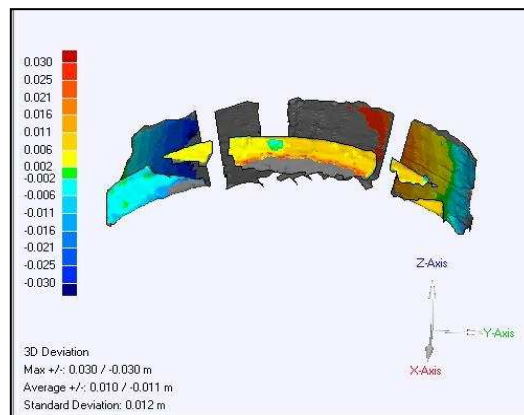


Fig 15. The oblique view of the 3D deviation of the tunnel crown (Chen, 2014)

Movement of the crown of the tunnel can be obtained by all 3 techniques and Table 2 gives results for the average value of movement from 3 points around the area of the crown using the physical model test (with mortar mix proportion 1:1:6) at the uniform load of 0kN and 590kN.

Table 2. Deformation results comparison at the crown

Measuring method	Crown coordinates from two measurement epochs			Average deformation (mm)
	X (mm)	Y (mm)	Z (mm)	
POT	N/A	N/A	N/A	27.14
	N/A	N/A	N/A	
Photogrammetry	-53.09	1058.14	239.79	35.63
	-52.06	1068.80	205.80	
Laser scanning	-1582.79	-109.38	535.60	40.10
	-1576.40	-104.43	495.37	

Although measurements were taken as quickly as possible it would be expected that the results between methods would suffer very slightly from settling in to equilibrium. As Table 2 displays, the results difference between potentiometers and photogrammetry was 8.5 mm while the difference between potentiometers and the laser scanner was up to 13 mm. The slightly small difference between photogrammetry and laser scanning is correlated with a closer time of measurement.

### Measurement of cracks

Crack measurements were analysed at the hinge failure at one third of the tunnel arch (with mortar mix proportion 1:2:9) under concentrated loading. Both the photogrammetry and the laser scanning techniques showed that they could be used for crack measurement. Fig. 16 and Table 3 (Chen, 2014) and Fig. 17 and Table 4 (Chen, 2014) show the images and measurements from a typical crack using photogrammetry and laser scanning respectively. Table 5 shows some manual vernier calliper measures as a contact measurement alternative at the same measurement positions. The crack lengths from these two remote techniques were measured three times to enable an average to be computed. This also gave an opportunity to assess the measurement quality. Tables 6 and 7 give a summary of the 3 techniques for comparison.

The spread of the crack length measurements from photogrammetry is 0.35mm; from laser scanning is 0.30mm and from the vernier callipers is 0.43mm. This probably highlights more of a problem with identification of what is the start and end of the crack rather than the accuracy of the measurement process.

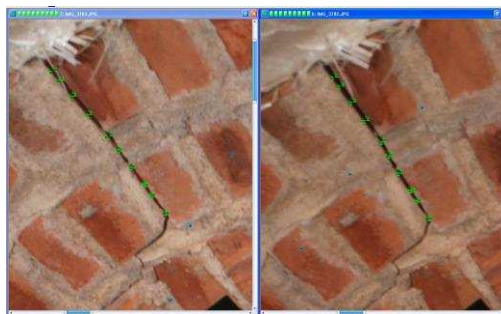


Fig 16. Non-targetted points of interest along a major crack used in photogrammetric measurement (Chen, 2014)

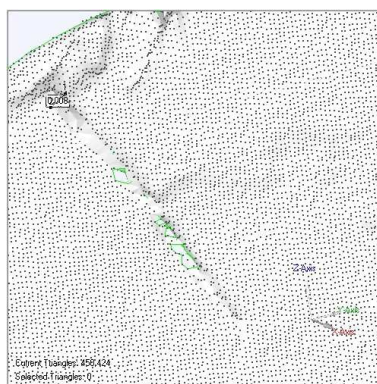


Fig 17. Cloud points along a major crack from the laser scanning technique (Chen, 2014)

Table 3. The major crack results by photogrammetry

Crack length No.	Crack length in each coordinate			Crack length (mm)
	$\Delta X$ (mm)	$\Delta Y$ (mm)	$\Delta Z$ (mm)	
1	54.29	58.45	66.15	103.63
2	53.79	59.06	66.32	103.83
3	52.43	60.04	65.99	103.48
Average	53.50	59.18	66.15	103.65
Position No.	Crack width in each coordinate			Crack width (mm)
	$\Delta X$ (mm)	$\Delta Y$ (mm)	$\Delta Z$ (mm)	
1 (The beginning position)	2.03	1.46	1.99	3.20
2 (The middle position)	1.46	2.57	2.34	3.77
3 (The end position)	0.63	1.26	1.35	1.80

Table 4. The major crack by the laser scanning technique

Crack length No.	Crack length in each coordinate			Crack length (mm)
	$\Delta X$ (mm)	$\Delta Y$ (mm)	$\Delta Z$ (mm)	
1	24.98	49.84	87.12	103.43
2	24.37	48.66	87.80	103.30
3	23.17	47.53	88.55	103.13
Average	24.17	48.68	87.82	103.29
Position No.	Crack width in each coordinate			Crack width (mm)
	$\Delta X$ (mm)	$\Delta Y$ (mm)	$\Delta Z$ (mm)	
1 (The beginning position)	4.62	2.09	1.94	5.43
2 (The middle position)	2.44	4.03	2.88	5.52
3 (The end position)	1.78	1.97	0.86	2.79

Table 5. The major crack by vernier calliper

Crack length No.	Crack length (mm)
1	103.34
2	103.65
3	103.22
Average	103.40
Position No.	Crack width (mm)
1 (The beginning position)	4.13
2 (The middle position)	4.33
3 (The end position)	2.78

A comparative study between different techniques is summarised in Tables 6 and 7. If the vernier calliper measurements are considered the benchmark for the crack lengths (Table 6) then laser scanning gives a slightly closer result than the photogrammetry. When considering the crack width the photogrammetry results are slightly closer to the vernier measurements at the beginning and middle position with the laser scanning closer at the end point.

Table 6. The major crack length results comparison (Chen, 2014)

Measuring method	Average distance in each coordinate			Average crack length (mm)
	X (mm)	Y (mm)	Z (mm)	
Vernier calliper	N/A	N/A	N/A	103.40
Photogrammetry	53.50	59.18	66.15	103.65
Laser scanning	24.17	48.68	87.82	103.29

Table 7. The major crack width results comparison (Chen, 2014)

Measuring method	The beginning position (mm)	The middle position (mm)	The end position (mm)
Vernier calliper	4.13	4.33	2.78
Photogrammetry	3.20	3.77	1.80
Laser scanning	5.43	5.52	2.79

## CONCLUSION

This study has shown that both photogrammetry and laser scanning are high accuracy measurement techniques suitable for monitoring displacements and crack sizes. Being remote measurement they provided a safe and relatively easy way of obtaining 3 dimensional movements. The quality of the results suffered from the physical identification or definition of the natural detail points typically produced in crack measurement. One big advantage of photogrammetry and laser scanning is the ability to produce 3D coordinates and 3D computer models. The results from both the remote measurement techniques were considered acceptable for use in the wider numerical modelling validation.

## ACKNOWLEDGEMENTS

This article is based on the paper presented at the 2nd Joint International Symposium on Deformation Monitoring (JISDM) held at The University of Nottingham on 9-11 September 2013 (Chen, 2013). The authors would like to thank the organiser of JISDM and Survey Review for the opportunity to present the work in the Survey Review journal.

## REFERENCES

1. BS4551:1980, 1980. Methods of testing mortars, screeds and plasters. London: British Standards Institution.
2. Chen H, Yu H, Smith M J, Kokkas N, 2013 Advanced monitoring techniques for assessing the stability of small-scale tunnels. 2nd Joint International Symposium on Deformation Monitoring (JISDM), The University of Nottingham on 9-11 September 2013.
3. Chen H, 2014. Physical Model Tests and Numerical Simulation for Assessing the Stability of Tunnels. PhD thesis, The University of Nottingham.
4. Faro, L., 2011. Laser Scanner Focus<sup>3D</sup> Technique Sheet.
5. Geomagic, Inc., 2007. Geomagic Studio 10 Software Manual, United States.



6. Guarnieri, A., Vettore, A. & Remondino, F., 2004. Photogrammetry and ground-based laser scanning: assessment of metric accuracy of the 3D model of Pozzoveggiani church. FIG Working Week 2004, 22-27.
7. Haack, A., Schreyer, J. & Jackel, G., 1995. State-of-the-art of Non-destructive Testing Methods for Determining the State of a Tunnel Lining. Tunneling and Underground Space Technology, 10, 413-431.
8. Idris, J., Al-Heib, M. & Verdel, T., 2009. Numerical modelling of masonry joints degradation in built tunnels. Tunnelling and Underground Space Technology, 24, 617-626.
9. Idris, J., Verdel, T. & Al-Heib, M., 2008. Numerical modelling and mechanical behaviour analysis of ancient tunnel masonry structures. Tunnelling and Underground Space Technology, 23, 251-263.
10. Kolymbas, D., 2005. Tunneling and tunnel mechanics: a rational approach to tunnelling, Springer Verlag.
11. Photometrix Pty Ltd., 2006. User Manual for Australis, Version 7.0., Australia.
12. Turner, A., Kemeny, J., Slob, S. & Hack, R., 2006. Evaluation, and management of unstable rock slopes by 3-D laser scanning. International Association for Engineering Geology and the Environment (IAEG), paper no. 404, Geol. Soc. London, pp. 1-11.